
ARTICLE

Digital two-parametric processing of the output data from radiation detectors

Zdenek Matej^{a*}, Moslem Amiri^a, František Cvachovec^b, Vaclav Prenosil^a, Filip Mravec^a and Zdenek Kopecky^c

^aFaculty of Informatics, Masaryk University, Brno, Czech Republic; ^bFaculty of Military Technology, University of Defense, Brno, Czech Republic; ^cVF, a.s., Cerna Hora, Czech Republic

In this paper, we present the results of digital processing of pulses produced by several types of detectors. We introduce a new high quality discrimination method, and the output from this new method is compared with those from classic methods. Also, a new function to determine separation quality of various discrimination methods is defined in this paper. Our results show how the quality of the particle type identification depends on the sampling rate as well as the method of sampled data processing.

Keywords: two-parameter spectrometer; digitalization; gamma/neutron distinguishing; neutron/gamma spectrum

1. Introduction

In digital discrimination of radiations, our purpose is to identify two characteristic parameters of the output pulses. One parameter is usually the pulse amplitude that contains information about the deposited particle energy to a detector. The other parameter can be the characteristic time constant of the leading or trailing edge of the pulse, whose value depends on the type of detected particles and allows distinguishing the components of mixed field made up of different types of particles.

2. Experimental equipment

2.1. Detectors

The pulse digitization has been studied for several detector types.

2.1.1 Stilbene and NE-213 organic scintillators

The physics of the different time response of the neutron versus photon scintillation is the same for the both scintillator types, being known for many years already [1].

2.1.2 ZnS(Ag) scintillator combined with a plastic scintillator

It is an alpha plus beta radiation detector. A plastic scintillator of a thickness of 0.25 mm (beta radiation detection) is coated with a ZnS(Ag) poly-crystalline layer [2]. When a low load resistance (50 Ω) is used in

the photomultiplier anode circuit, the voltage pulse decay time comes up to the scintillation decay time. In the cases of the plastic and the ZnS(Ag) scintillators, it equals 2.4 ns and 200 ns, respectively (**Figure 4**).

2.1.3 Hydrogen-filled proportional detector

It is a spherical detector operating with a pressure of 404 kPa. The discrimination between neutron and photon pulses is based on dissimilar linear stopping powers of secondary particles arising from the interaction of neutrons in the gas filling and photons in the metallic cathode and gas filling, i.e., protons and electrons. The range of track length of a proton is shorter than that of an electron. The ionization is taken place by a proton in narrower region than that by an electron. Therefore, the induced current signal by a proton has faster leading edge than electron.

2.1.4 Digitized apparatus

The block diagram of the digitized apparatus is in **Figure 1**.

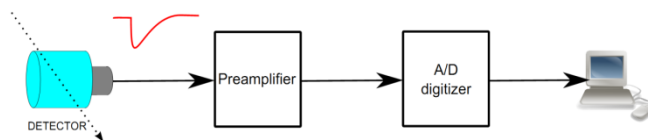


Figure 1. Block diagram of a digital two-parameter analyzer.

We used two commercially available Agilent digitizers to digitize the output pulses; DP 210 type featured up to 2 GS/s, bandwidth 500 MHz and 8 bits, whereas the maximum sampling frequency of the

*Corresponding author. Email: xmatej@fi.muni.cz

DC 222 type amounted to 8 GS/s, bandwidth 1 GHz at a 10-bit resolution.

Two variants of the anode load resistance were tested in conjunction with the scintillation detectors. In the first variant, a load resistance of 40 kΩ was used. Different waveforms of the neutron and photon pulses can be found in the voltage pulse leading edge (Figure 2). If the magnitude of the load resistance is selected 50 Ω, the different shape of the neutron/photon pulse will appear to take effect on the decay time. The organic scintillator and the detector consisting of the plastic scintillator combined with ZnS(Ag) were connected in this way (Figure 3 and Figure 4).

The output resistance of the hydrogen-filled proportional detector is of the order of MΩ. The difference between the neutrons versus photon waveforms consists again in the rise time.

3. Data evaluation

3.1. Particle type resolution by the rise time

In rise time technique [3,4], the difference in pulse leading edges is used for discrimination. As a criterion for discriminating between the neutron and photon pulses, the time elapsed between the instants at which the pulse reaches the p-th and q-th parts of its amplitude can be used in the simplest case. It has been found experimentally that p=0.1 and q=0.9 can be chosen.

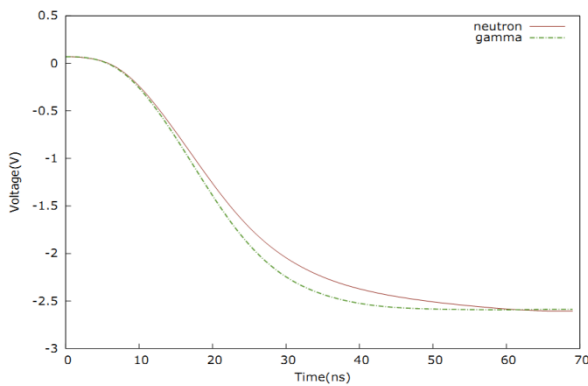


Figure 2. The photon and neutron pulse shape in the anode circuit for a large load resistor (stilbene scintillation detector).

3.2. Particle type resolution by the decay time

There are several processing algorithms available. One of them is the pulse part integration method. In this case, the processing method proves to be useful, which consists in comparing the ratio r of integrals of the voltage pulse waveforms, as Eq. (1) indicates:

$$r = \frac{\int_{\tau_1}^{\tau_3} u(t).dt}{\int_{\tau_2}^{\tau_3} u(t).dt} \quad (1)$$

where τ_1 is the voltage pulse start time, τ_3 is the pulse end time and τ_2 is an empirically identified point

between τ_1 and τ_3 , at which the neutron pulse trailing edge starts to differ from that of the photon one. The values τ hold $\tau_1 < \tau_2 < \tau_3$. For a stilbene scintillator, the parameter r equals 110 and 70 for neutrons and photons, respectively.

This processing method also works well when identifying the pulses produced by an alpha and beta scintillator consisting of a plastic scintillator layer (beta) and ZnS(Ag) scintillator (alpha). The pulse waveforms are shown in Figure 4.

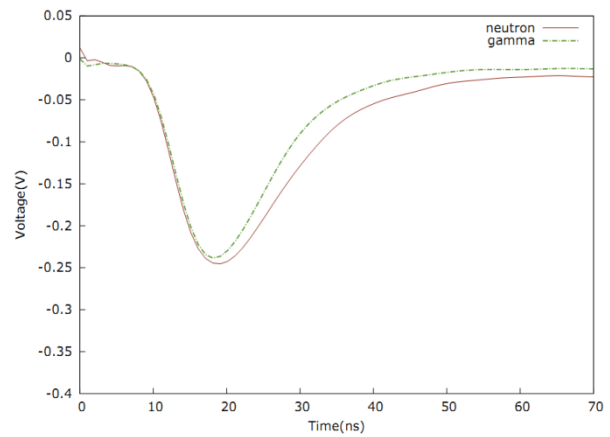


Figure 3. Shape of photon and neutron pulses in the photomultiplier anode circuit for 50 Ω load resistor (stilbene scintillation detector).

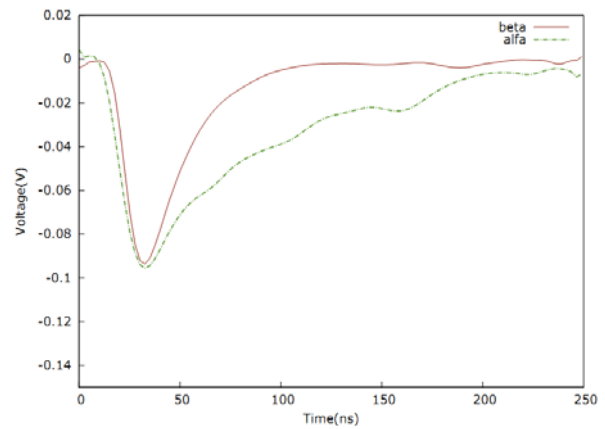


Figure 4. Waveforms of alpha and beta radiation pulses at the photomultiplier output of the ZnS(Ag) and plastic detector.

3.3. Distinguishing neutrons from photons by means of the Mean vs. Square Standard Deviation method

Working on the features of the neutron and gamma signals reveals that the mean vs. square standard deviation (μ vs. σ^2) plot of the samples of each radiation type falls in a completely separate area in the coordinate system.

The mean of a signal contained in x_0, x_1, \dots, x_{N-1} is calculated as:

$$\mu = \frac{1}{N} \sum_{i=0}^{N-1} x_i \quad (2)$$

and the square standard deviation as:

$$\sigma^2 = \frac{1}{N-1} \sum_{i=0}^{N-1} (x_i - \mu)^2 = \frac{1}{N-1} \left[\sum_{i=0}^{N-1} x_i^2 - \frac{1}{N} \left(\sum_{i=0}^{N-1} x_i \right)^2 \right] \quad (3)$$

Since the number of samples for every signal is constant in an experiment of neutron and photon discrimination, on receiving every new sample of a signal, only two parameters need to be updated:

- The sum of the samples received so far;
- The sum of square of the samples received so far.

4. Off-line and on-line processing of digital data

The sample count is of several tens up to a maximum of 400. Together with the processing method, this imposes relatively high demands on the performance of the computing machinery when operating on-line. On the other hand, it offers a range of benefits, such as data storage and off-line processing at a later time by different methods.

4.1. Off line processing

The processing takes place in several independent steps. First of all, physical measurement is carried out in the required range. The next step is processing these data by means of the above-mentioned algorithms with the aim of finding the spectral distribution. In the steps to follow, this output is to be divided into the neutron and photon spectra, which are subsequently recalculated, depending on the detector type and its response, to give the required result. This procedure results in energetic spectra of neutrons and gamma radiation.

4.2. On line processing

We created an application for this procedure which is capable to initialize the respective digitizer, set up the required parameters and, finally, read the measured pulses repeatedly. The digitizers allow the experimenter to use two types of data transmission into the computer memory. They are either repeated reading of separate pulses (so-called segments) or one-shot transmission of several segments into the memory by means of Direct Memory Access (DMA). The second option is obviously more memory demanding, however, it is time-saving if a large quantity of segments is to be read. On the other hand, the first option is faster provided that a single segment includes a large quantity of samples. In our case, the second option is more advantageous in most cases.

For on-line processing, we are using the various algorithms described in paragraphs 3.1 through 3.3.

5. Results

5.1. Separation quality function, $F(u)$

In this paper, we introduce a new separation quality function, $F(u)$, as a means for comparison of various discrimination methods. In a three dimensional coordinate system, with x , y , and z axes representing “particle type distinguishing parameter”, “pulse

amplitude u ,” and “number of pulses $n(u)$,” respectively, for pulses with amplitudes higher than a specific level (called level 0), $F(u)$ is calculated as follows:

$$F(u) = \frac{\Delta_{ab}}{\Delta_a + \Delta_b} \frac{N'(u)}{N(u)} \quad (4)$$

where $N(u)$ is the number of pulses whose amplitudes are above the level 0, $N'(u)$ is the number of pulses whose amplitudes are between level 0 and the amplitude of the valley between the two fitted Gaussian plots to the two radiations (called level $n(u)$), Δ_a and Δ_b are the distances between the first occurrence of the minimum value between peaks and the corresponding peak, and Δ_{ab} is the distance between the two peaks. $F(u)$ can be defined for various level-0s. Diagram of **Figure 5** illustrates the application of this function on the fitted Gaussian plots of two radiations in the coordinate system (the third dimension, $n(u)$, is not shown here.) If $n(u) = 0$ in the minimum part between the peaks, the peaks of a , b , particles are separated perfectly; $n(u) > 0$ in a minimum between the peaks corresponds to the section in the areas of imperfect separation of the particle types.

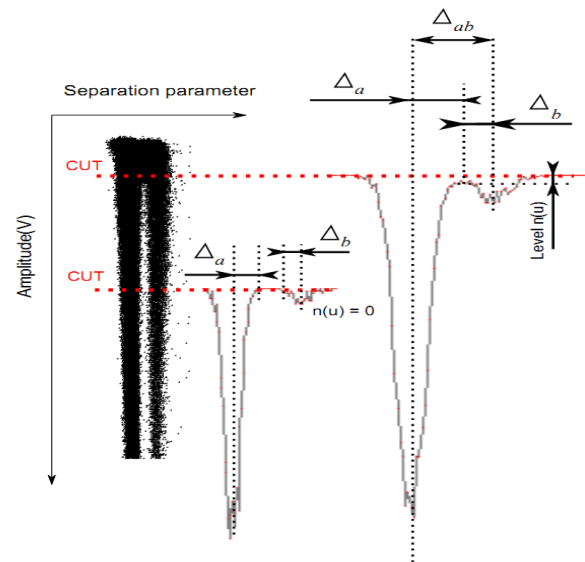


Figure 5. On the quality function definition.

It follows from the definition that the particles a , b , are separated from each other imperfectly for $F(u) < 1$. For $F(u) > 1$ they are separated from each other quite well.

5.2. Particle type separation for particular detector types

5.2.1 Stilbene scintillator

The quality of the neutron / photon separation using method 3.1 is shown in **Figure 6** for mixed field of a Cf neutron source. Figure 6 and the following shows the limit for $F(u) = 1$ below which neutrons and photons are not well separated. The load resistor in the photomultiplier anode circuit was 40 k Ω and the difference in the rise time of the neutron / photon pulse (Figure 2).

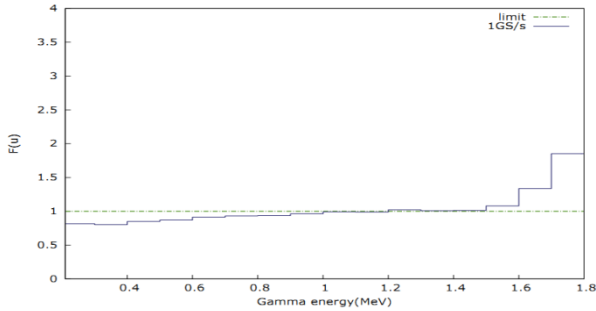


Figure 6. Neutron / gamma separation quality function $F(u)$ for stilbene scintillator by the pulse leading edge - method 3.1.

Figure 7 shows the resolution function for a load resistance of 50Ω in the photomultiplier anode circuit, the pulse sampling rate being set to 4 GHz. The output pulse shape is shown in Figure 3. The 45×45 mm stilbene detector output data were evaluated by means of method 3.2.

It follows from the shape of $F(u)$ functions in Figure 6 and Figure 7 that the n/gamma resolution obtained from the decay time by means of the integration method is better than that from the pulse leading edge.

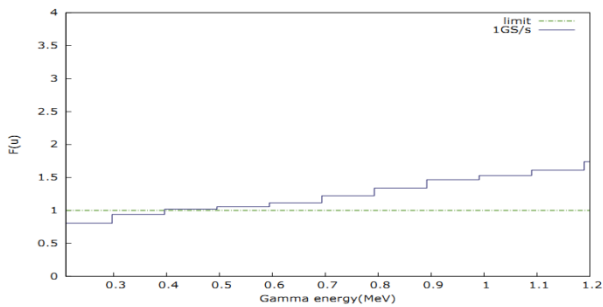


Figure 7. Separation function $F(u)$ for stilbene n / gamma scintillator by the pulse trailing edge method 3.2.

5.2.2 Dependence of the $F(u)$ on the effect of the sampled data processing method

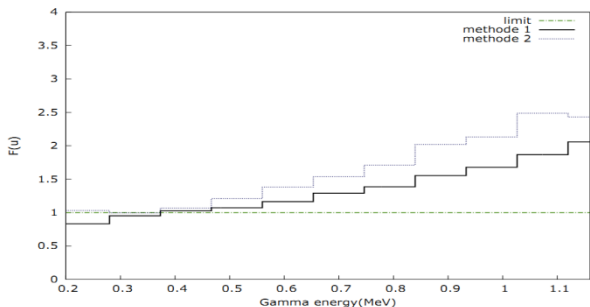


Figure 8. Comparison of the results of the methods specified in sections 3.2 and 3.3 for the same data. Sampling frequency was 4GS / s.

Figure 8 shows the same data as above but obtained by stilbene scintillator from Cf source and a load resistor of 50Ω using the methods 3.2 (curve 1) and 3.3 (curve 2). Method 3.3 appears to be somewhat more efficient.

5.2.3 Dependence of the $F(u)$ on the effect of the digitizer sampling rate

Figure 9 shows how the pulse separation depends on the data obtained by measuring the Cf source using different digitizer sampling rates, under identical measurement conditions. Method 3.2 was used to evaluate the n/gamma separation. It is seen from the Figure that higher sampling rates lead to substantially better results. The duration of the pulse is sampled approximately 25 ns. If we get under 250 MHz sampling time can not be longer pulses well separated in small energy.

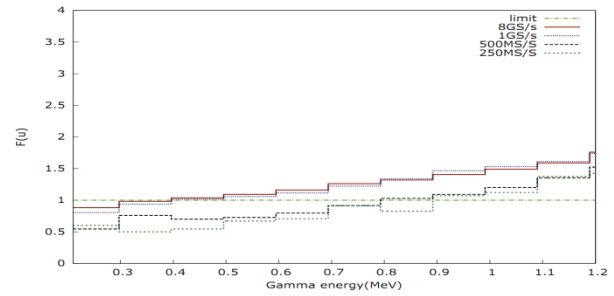


Figure 9. Comparison of results obtained when using different sampling frequencies.

5.2.4 NE-213/BC501A, neutron / photon separation

Figure 10 shows the $F(u)$ function for NE-213 detector of dimensions 76.2×76.2 mm. As a source of the neutron / gamma mixed field a Cf source was used. Digital data were evaluated by means of the 3.2 method. The neutron / gamma resolution is seen to be excellent.

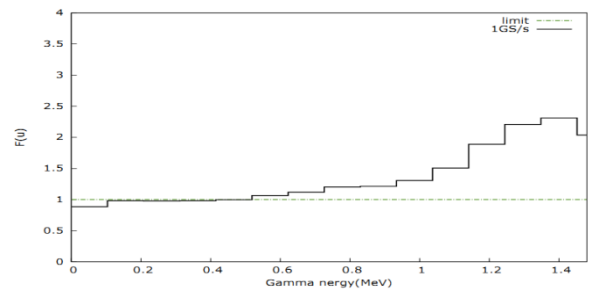


Figure 10. NE213/BC501A, sampling rate 1GS/s.

5.2.5 Plastic/ZnS(Ag) scintillation detector, beta/alpha separation

The integration method described in paragraph 3.2 was used to process the data. 2D diagram (**Figure 11**) was used to illustrate the results. ^{241}Am and ^{90}Sr were used as a source of alpha and beta particles.

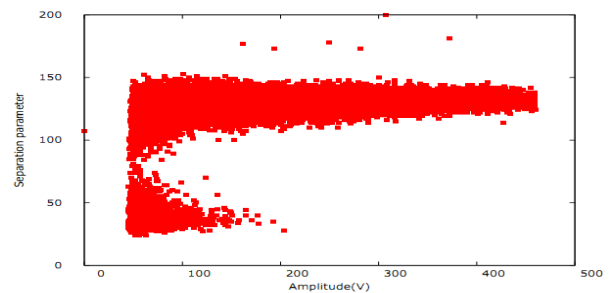


Figure 11. Processing result of alpha and beta mixed field.

5.2.6 Hydrogen-filled proportional detector, neutron / photon separation

Digitized output pulses of the hydrogen-filled proportional detector were processed by the method described in paragraph 3.1. It is to be noted that the neutron pulses arise from recoil protons, whose linear stopping power exceeds that of electrons by means of which the photons are detected. Therefore, the pulses corresponding to the shorter charge collection in **Figure 12a** correspond to photons from ^{137}Cs and ^{60}Co . **Figure 12b** shows the 2D distribution of pulses from ^{252}Cf neutron and photon source.

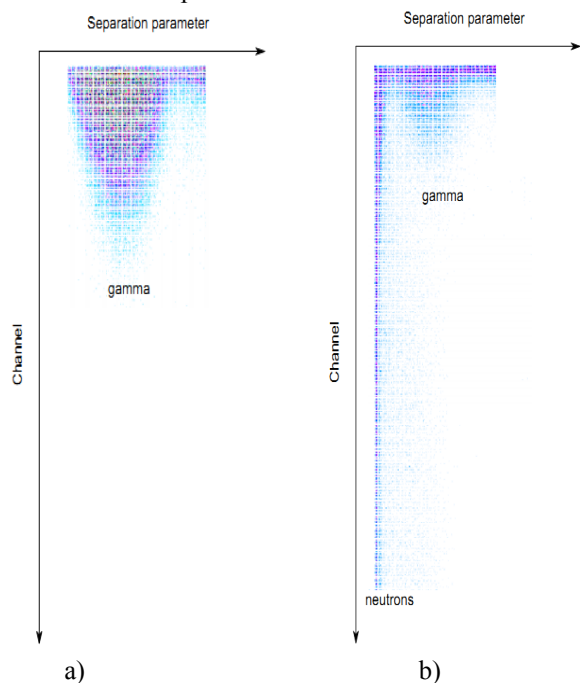


Figure 12a. Distribution of pulses from ^{60}Co and ^{137}Cs , 12b. Distribution of pulses from ^{252}Cf source

6. Conclusion

Our results show the digital processing of pulse detector output data to be a largely useful and promising technique. Experiments have proved that a sufficiently powerful digitizer is able to work together with pulse detectors of most diverse types. The sampling rate and the quantization level resolution make the decisive parameters. The selection of the most suitable sampling rate is closely related to the duration of the pulse sampled part. Based on our experience, the sampling period should not exceed 10 % of the duration of the pulse sampled part. Better results can be achieved by its shortening i.e. by using a higher sampling rate. In the case of the detectors used in our experiments, we had to

use a sampling rate of 1 GHz at least. The higher are the energy resolution and the width of the energy interval required, the more severe are the demands on the quantization level resolution. In the case of organic scintillators and type Cf neutron spectra measurements, the spectrum is to be measured in two parts when a 10-bit digitizer is used. 12-bit digitization is fully satisfactory.

Acknowledgment

The work presented in this paper has been supported in the framework of specific research of the Department of Mathematics and Physics, University of Defense Brno in 2011 and research project SPECTRUM, No. TA01011383 of the Technology Agency of the Czech Republic.

References

- [1] G. F. Knoll, *Radiation Detection and Measurement*, third edition, John Wiley & Sons, Inc, (2000), ISBN-0-47-0738-5.
- [2] EJ-444 Dual Phosphor Thin Scintillator, www.eljentechnology.com
- [3] T.K. Alexander and F.S. Goulding, An amplitude-insensitive system that distinguishes pulses of different shapes, *Nuclear Instruments and Methods*, 13, (1961), pp. 244-246, ISSN 0029-554X.
- [4] M.L. Roush, M.A. Wilson and W.F. Hornyak, Pulse shape discrimination, *Nuclear Instruments and Methods*, 31, (1), (1964), pp. 112-124, ISSN 0029-554X.
- [5] F.D. Brooks, A scintillation counter with neutron and gamma-ray discriminators, *Nuclear Instruments and Methods*, 4(3), (1959), pp. 151-163.
- [6] J.M. Adams and G. White, A versatile pulse shape discriminator for charged particle separation and its application to fast neutron time-of-flight spectroscopy, (<100 keV – 20 MeV), *Nuclear Instruments and Methods*, 156(3) (1978), pp. 459-476.
- [7] J. Cvachovec and F. Cvachovec, Maximum likelihood estimation of a neutron spectrum and associated uncertainties, *Advances in Military Technology*, 3(2) (2008), pp. 67-79.
- [8] G. Liu, M.J. Joyce, X. Ma and M.D. Aspinall, A digital method for the discrimination of neutrons and rays with organic scintillation detectors using frequency gradient analysis, *IEEE Transactions on Nuclear Science*, 57(3) (2010), pp. 1682-1691.